ISSN 0915-033X

Beta-Limiting Phenomena in High-Aspect-Ratio Toroidal Helical Plasmas

K. Itoh, A. Fukuyama and S.-I. Itoh

(Received – Aug. 31, 1992)

NIFS-188 Oct. 1992

RESEARCH REPORT
NIFS Series

This report was prepared as a preprint of work performed as a collaboration research of the National Institute for Fusion Science (NIFS) of Japan. This document is intended for information only and for future publication in a journal after some rearrangements of its contents.

Inquiries about copyright and reproduction should be addressed to the Research Information Center, National Institute for Fusion Science, Nagoya 464-01, Japan.

NAGOYA, JAPAN

Beta-Limiting Phenomena in High-Aspect-Ratio Toroidal Helical Plasmas

K. Itoh*, A. Fukuyama**, S.-I. Itoh+

* National Institute for Fusion Science, Nagoya 464-01, Japan

** Faculty of Engineering, Okayama University, Okayama 700, Japan

+ Research Institute for Applied Mechanics, Kyushu University 87, Kasuga 816, Japan

Keywords: Beta Limit, Sawtooth, Helical System, Interchange Mode, High Aspect Ratio, Magnetic Hill

Abstract

Evolutions of the local pressure gradient and the amplitude of the helical mode are studied near the critical pressure gradient against the linear resistive interchange instability in the high aspect ratio toroidal helical plasmas. Three characteristic dynamic evolutions are identified; monotonous saturation, relaxation oscillation and periodic limit cycle solution. As the heating power is increased, the dynamic evolution changes from the monotonous saturation, to the relaxation ocsillation and finally to the limit cycle. The time average of the pressure gradient is limited by the critical gradient against the linear stability. Dependences of the amplitude and period of the sawtooth oscillation on the heating power are also analyzed.

§1. Introduction

Recently much work has been performed to investigate the stability limit against the interchange mode (Rosenbluth and Longmire, 1957) in stellarators with the finite shear and magnetic hill such as Torsatron/ Heliotron devices (Gurldon, et al., 1968; Mohri, 1970; Uo, 1971). Compared to the flourishing work on the linear stability problem, few theoretical investigations have been made on the process which really limits the achievable β limit. (β value is the ratio of the plasma pressure to the magnetic pressure.) The sawtooth-like oscillation is known to appear when plasma pressure increases (Harris, et al., 1984). Wakatani and coworkers have performed a numerical simulation for the resistive interchange mode to simulate it (Wakatani, et al., 1984). However, the sawtooth oscillation does not necessarily appear in experiments at beta limit (Morimoto, et al., 1989). In addition to it, the resistive MHD calculation predicts instability for all values in this geometry (Ichiguchi, et al., 1989, 1991), the concept of the 'beta limit' is not clear. The analysis on the beta-limiting phenomena in this configuration has been far from satisfactory.

We have recently developed the analytical theory on the stability of the interchange mode in the high-aspect-ratio Torsatron/Heliotron configurations, taking into account of the plasma dissipation such as the resistivity, η, thermal conductivity, χ, current diffusivity, λ, and ion viscosity, ν (Itoh, et al., 1992b). It was found that the small but finite value of thermal conductivity and ion viscosity is essential in

determining the stability β-limit (Itoh, et al., 1992b, Carreras, et al., 1987). In this article, we extend this analysis and study the temporal evolution of the mode amplitude and the pressure gradient. The dynamics of the pressure gradient and the mode amplitude are studied by taking into account the background profile modification. This model reveals the periodic sawtooth-like oscillation with the bursts of the perturbation amplitude. Other types of the solutions, such as the monotonous saturation or the relaxation oscillatiion are also found. The boundary in the parameter space for these types of solution is also obatined. We also investigate the peak value and the time-averaged value of the pressure gradient as a function of the heating power, and illustrate how they are limited by the evolution of the low-poloidal mode number interchange mode.

§2. Model

(2.1) Growth Rate of the Interchange Mode

We use a model equation based on the reduced set of equations for stellarators (Strauss, 1980). High-aspect-ratio plasma is analyzed to obtain the analytic insight. The cylindrical geometry with the coordinates (r, θ, z) is employed.

The growth rate γ of the resistive interchange mode, which is localized near the mode rational surface, is derived as (Itoh, et al., 1992b)

$$\tau = \left[\frac{64Dk_\theta^2\chi^2}{\nu}\right]^{1/3} \exp\{-\frac{\pi s}{2}\sqrt{\frac{\chi}{D\eta}}\} - \chi k_\theta^2 \qquad (1)$$

where $k_\theta = m/\rho_1$, m is the poloidal mode number, ρ_1 is the normalized minor radius of the mode rational surface, s is the shear parameter, $\rho_1(\partial\iota/\partial\rho)/\iota$, D nenotes the normalized pressure gradient

$$D = -\Omega' \beta p'_{eq}, \qquad (2)$$

$' \equiv \partial/\partial\rho$, p_{eq} is the normalized pressure, $p(r)=[\beta p_{eq}(\rho)]B^2/2\mu_0$ and Ω' is the averaged curvature of the field lines. In Eq.(1), τ, η, χ, and ν are normalized to τ_A, $a^2\mu_0/\tau_A$, a^2/τ_A, and a^2/τ_A, respectively. (a is the plasma minor radius.) In the following, the length and time are nornalized to a and τ_A, unless specified otherwise.

Equation (1) predicts that $\tau=0$ at critical values of D, which we denote by D_c. The critical pressure gradient, D_c, is given as (Itoh, et al., 1992b; Carreras, et al., 1987)

$$D_c = \left[\frac{3\pi s}{2}\right]^2 \frac{\chi}{\eta}\left[\ln\{\left[\frac{3\pi s}{2}\right]^2 \frac{1}{\nu\eta k_\theta^4}\} - 2\ln\left|\ln\{\frac{\chi\nu k_\theta^6}{64}\}\right|\right]^{-2}. \qquad (3)$$

In the vicinity of the stability boundary, we write

$$\tau = [\partial\tau/\partial D](D-D_c). \qquad (4\text{-}1)$$

and

$$\frac{\partial \tau}{\partial D} = \left[\frac{64 k_\theta \chi^2}{D^2 \nu}\right]^{1/3} \exp\left[-\frac{\pi s}{2}\sqrt{\frac{\chi}{D\eta}}\right]\left[\frac{1}{3} + \frac{\pi s}{4}\sqrt{\frac{\chi}{\lambda D}}\right] \qquad (4\text{-}2)$$

Figure 1 shows an example of the growth rate as a function of the pressure gradient.

(2.2) Evolution of Pressure Profile

We next introduce the model equation for the evolution of the local pressure gradient. The evolution of the averaged pressure profile, $p(\rho)$, is given as

$$\partial p/\partial t = \chi \nabla^2 p - \langle \tilde{v} \cdot \nabla \tilde{p} \rangle, \qquad (5)$$

where $\tilde{}$ denotes the perturbation, $\langle\ \rangle$ indicates the time-phase average, and the contribution of the local heating power is neglected. The second term indicates the quasilinear term corresponding to the convective flattening of the background profile. We here assume that χ is constant in space and time for the simplicity. The perturbation of the pressure $\tilde{p}$ is related to velocity perturbation $\tilde{v}$ as

$$\tilde{p} = -\frac{\tilde{v} \cdot \nabla p}{\tau + \chi k^2} \qquad (6)$$

Substituting Eq.(6) into Eq.(5), we have

$$\frac{\partial p}{\partial t} = \nabla \chi \nabla p + \frac{\langle \tilde{v} \cdot \nabla \tilde{v}_r \rangle}{\tau + \chi k^2} \nabla p \ . \qquad (7)$$

The development of the averaged pressure gradient is given by

$$\frac{\partial}{\partial t}(\nabla p) = \nabla^2 \chi(\nabla p) + \frac{\nabla\langle \tilde{v}\cdot\nabla\tilde{v}_r\rangle}{\tau+\chi k^2}(\nabla p) \ . \tag{8}$$

The boundary condition is chosen that the heat flux (supplied by the external heating method) is constant in time far from the region in which this low-m mode activity exist.

We develop the point model in order to keep the analytic insight of the phenomena. We assume that the perturbation is localized near the mode rational surface, and introduce the scale length of ℓ, which shows the localization width of the pertubation. For the analytical insight, we assume the scale length separation, i.e., $\ell|\nabla p/p|<<1$ and $\ell k \sim O(1)$. By using this model, we estimate as

$$\nabla\langle \tilde{v}\cdot\nabla\tilde{v}_r\rangle\nabla p \simeq (\nabla p)\cdot\nabla\langle \tilde{v}\cdot\nabla\tilde{v}_r\rangle \tag{9}$$

and

$$k^2 = k_\theta^2 + 1/\ell^2. \tag{10}$$

The derivative on the perturbation quantity is estimated as

$$\nabla\langle \tilde{v}\cdot\nabla\tilde{v}_r\rangle \simeq |\tilde{v}_r^2|/2\ell^2 \tag{11}$$

The contribution of the diffusion term (the first term in RHS of Eqs.(7) and (8)) is evaluated in the point model by noting the boundary condition. Since the heat flux and χ is constant at $|\rho-\rho_f|>>\ell$, we use the condition

$$\nabla p = \nabla p_{heat} \quad \text{at} \quad |\rho-\rho_f|>>\ell, \tag{12}$$

and ∇p_{heat} is constant in time. By the help of this condition, the second derivative of ∇p is evaluated by

$$\nabla^2(\nabla p) \simeq \ell^{-2}(\nabla p_{heat}-\nabla p). \tag{13}$$

The diffusion term is usually characterized by the loss time τ. We introduce τ as $1/\tau = \chi/\ell^2$ and use the notation as

$$\nabla^2\chi\nabla p = (\nabla p_{heat} - \nabla p)/\tau. \tag{14}$$

Note that ∇p_{heat} is the pressure gradient which is realized by the balance between the heating and the diffusive loss. In other words, ∇p_{heat} is the pressure gradient which would be realized in the absence of the low-m mode activity. Substituting Eqs. (9), (11) and (14) into Eq.(8) the model equation which dictates the evolution of the pressure gradient is obtained. Noting the relation between D and ∇p, we write this equation in terms of D as

$$\frac{dD}{dt} = \frac{1}{\tau}(D_{heat} - D) - \frac{D|\tilde{v}_r^2|}{2(\ell^2\tau+\chi)} \tag{15}$$

(The contribution of the external heating, D_{heat}, is defined as $D_{heat}/\nabla p_{heat}=D/\nabla p$.)

Using the growth rate τ, the time evolution of $|\tilde{v}_r^2|$ is given as

$$d|\tilde{v}_r^2|/dt = 2\tau\,|\tilde{v}_r^2|. \tag{16}$$

Equations (1), (15) and (16) constitute the set of basic equations.

§3. Temporal Evolution and Beta-Limiting Phenomena

(3.1) Dimensionless Form of Equation

Equations (1), (15) and (16) is solved to study the beta limiting phenomena near the critical beta value for the stability. In order to simplify the analysis, we use a normalized form as $F \equiv D/D_c$, $K \equiv \ell^2\langle\tilde{v}_r^2\rangle/\chi^2$ and $t \equiv t/\tau$, we have

$$\frac{dF}{dt} = (F_{heat} - F) - \frac{KF}{2+2\hat{\tau}} \tag{17}$$

and

$$dK/dt = 2\hat{\tau}K \tag{18}$$

where the normalized growth rate $\hat{\tau}$ is defined as $\tau\tau$. The Taylor expansion of τ, Eq.(3) is rewitten as

$$\hat{\tau} = z(F-1) \tag{19}$$

where the parameter z is defined as

$$z \equiv (\partial\tau/\partial D)D_c\ell^2/\varkappa. \tag{20}$$

Solution of Eq.(17) and (18) is investigated for the given parameters (F_{heat}, z).

(3.2) Fixed Point and Stability

Equations (17) and (18) have the fixed points. Setting d/dt=0, we have the fixed points (F_*, K_*) as

$$F_* = F_{heat}$$
$$K_* = 0 \tag{21-1}$$

and

$$F_* = 1$$
$$K_* = 2(F_{heat}-1). \tag{21-2}$$

The former solution corresponds to the case of low heating power,

i.e., $F_{heat}<1$ (in other words, $D_{heat}<D_c$). When heating power increases and F_{heat} exceeds unity, Eq.(21-1) denotes the unstable fixed point. The mode grows and the fixed point is given by Eq.(21-2), for which F_* is independent of D_{heat}, i.e., the pressure gradient is limited to the critical value against the linear stability.

The dynamical stability of the fixed point is studied by expanding Eqs.(17) and (18) near the fixed point. We write

$$F = F_* + f \text{ and } K = K_* + h \tag{22}$$

and linearlize Eqs. (17) and (18) as

$$\frac{d}{dt}\begin{bmatrix} h \\ f \end{bmatrix} = \begin{bmatrix} 0 & 2zK_* \\ -1/2, & -1+K_*(z-1)/2 \end{bmatrix} \begin{bmatrix} h \\ f \end{bmatrix} \tag{23}$$

The eigenvalue of the matrix, Λ, is given as

$$\Lambda = \frac{-\Gamma \pm \sqrt{\Gamma^2 - 4zK_*}}{2} \tag{24-1}$$

where

$$\Gamma \equiv 1 - K_*(z-1)/2. \tag{24-2}$$

The deviation from the fixed point, (h, f), change in time as $(h, f)=(h_0, f_0)\exp(\Lambda t)$. There are three cases depending on the

value of Λ. When Λ is real and negative, i.e.,

$$\Gamma^2 > 8z(F_{heat}-1), \text{ and } \Gamma>0, \tag{25}$$

the fixed point is stable. The trajectory (F,H) converges to the fixed point (F_*, K_*) without oscillation. If Λ is complex and *Re* $\Lambda < 0$, the fixed point has an asymptotic stability. (If the imaginary part is large, $|Im\,\Lambda| > |Re\,\Lambda|$, the trajectory oscillates aroung the fixed point many times on the path of convergence.) When the real part of Λ is positive,

$$K_*(z-1) > 2 \tag{26}$$

the fixed point is not stable, and the trajectory turns into the limit cycle. Near by the threshold condition, the frequency of the temporary oscillation, ω, is given as

$$\omega = \sqrt{\Gamma^2-4zK_*}/2. \tag{27}$$

Figure 2 illustrates these typical cases. In the first case, Λ is real and negative; F and K converges to the fixed point and the monotonic saturation is obtained. In the second case, i.e., *Re* $\Lambda<0$ and $|Im\,\Lambda|$ dose not vanish, the overshoot of F and K is obtained on the way of the asymptotic convergence. The instantaneous peak value of the pressure gradient can exceeds the critical value. In the third case, where *Re* $\Lambda>0$, the limit cycle solution occurs; the pressure gradient shows the sawtooth-like

oscillation, and the perturbation shows the periodic bursts. In this case, the instantaneous peak value of the pressure gradient can also exceeds the critical value. Figure 3 shows the regions of these solutions in the parameter space of F_{heat} and z.

(3.3) Numerical Example

Equations (17) and (18) are solved numerically. In performing the calculations, we choose parameters z and $k_\theta^2 \ell^2$. Combinations of η and χ are chosen so as to give the asigned value of z. Figure 4 illustrates three typical solutions, i.e., saturation, relaxation oscillation and limit cycle oscillation. The analysis based on the stability of the fixed points is confirmed. In the case of the damped oscillations, the first peak of the pressure gradient is largest. In high heating cases, the sawtooth oscillation of the pressure gradient is realized. As the heating power increased and the pressure gradient tends to exceed the stability limit, then the mode amplitude starts to grow. The increased perturbation stops the increment of the pressure gradient and causes its collapse. As the pressure gradient is flattened, the mode becomes stable and the mode amplitude starts to decrease. Then the pressure gradient starts to grow again, allowing the periodic changes.

Figure 5 shows how the pressure gradient and the perturbation amplitude change as the heating power is increased. Bold line indicates the time avarage of the pressure gradient in the stationary solutions. Below the critical value, $F_{heat}<1$, plasma is stable, and F grows in proportion to F_{heat}. If F_{heat}

exceeds unity, the plasma enters into the unstable region. It is found that the instantaneous peak value of the pressure gradient increases as the heating power increases, though much slower than F_{heat} itself. However, the dynamics of the trajectory (F,K) is asymptotically stable, and the pressure profile finally reduxces to a constant value, which is the critical pressure gradient, D_c. When the heating flux exceeds the criterion Eq.(26), or

$$\frac{\nabla p_{heat}}{\nabla p_c} > 1 + \frac{1}{D_c \partial\tau/\partial D - 1}, \tag{28}$$

where ∇p_c is the critical pressure gradient against the linear stability. The stationary solution turns to be the limit cycle, and pressure gradient F shows the sawtooth-like oscillation. The time-averaged value of the gradient is suppressed below the critical value against the linear stability. The peak and bottom of the periodic oscillation is also plotted in Fig.5 by dashed lines. The difference between the peak and bottom indicates the magnitude of the sawtooth crash. The crash amplitude $\Delta A/A$ is defined as

$$\Delta A/A \equiv |\nabla(\text{peak}) - \nabla p(\text{bottom})| / |\nabla p_c| \tag{29}$$

and it scales as

$$\Delta A/A \propto \sqrt{F_{heat}{}^{-1} - 1/(z-1)}. \tag{30}$$

The instantaneous peak of the pressure gradient exceeds the

stability limit D_c, but cannot surpass D_c much.

The mode amplitude is also shown in Fig.5. Below the criterion Eq.(28), the saturation amplitude is given by Eq.(21-2). When the parameters enters in the regime of the limit cycle oscillations, the mode amplitude rapidly increases.

The period of the oscillation is also studied as a function of the heating power. Figure 6 illustartes the period as a function of the heat flux parameter D_{heat}/D_c. When F_{heat}^{-1} is close to zaro, the oscillation frequency is close to the value given by Eq.(27). As the heat flux increases, the peak value of the mode amplitude increases very rapidly. Pressure gradient is depressed much. In the range $|D/D_c-1|>(\ell^2 k_\theta^2/z)$, the damping rate of the mode is approximated as

$$\tau \simeq -\chi k_\theta^2. \tag{31}$$

The damping rate remains close to this value until D approaches to D_c as is shown in Fig.1. The decay time of the pulse of the mode amplitude is estimated by $\ell^{-2}k_\theta^{-2}$ in the normalized form. This value is usually much larger than unity . In such a case, the contribution of the decay time in the period of oscillation is large and dominant. The period approaches to the value which is order of $\ell^{-2}k_\theta^{-2}$. ω is close to unity, and the period is an increasing function of the heat flux D_{heat}.

§4. Summary and Discussion

In this article, we developed the analytic theory of the

dynamic evolution of the plasma pressure gradient and the interchange mode amplitude near the stability boundary. A simplified set equation for the mode amplitude and pressure gradient was derived where the quasilinear back-ground modification is taken into account.

The dynamical evolution is studied, and we found that there are three classes of evolutions; the monotonic saturation, the relaxation oscillation and periodic limit cycle solution. The parameter region for the appearance of these solutions is also obtained. As the heating power is increased and the plasma enters into the unstable region, the saturation is realized when the heating power is not strong enough. As the heating power is increased, then the relaxation oscillation occurs; in this case, the overshoot of the pressure gradient is predicted. The pressure gradient shows the sawtooth-like oscillation, the amplitude of which is largest for the first crash, and converges to the saturation value with reduced oscillation amplitude. Finally, if the heating power is large enough, the periodic sawtooth-like oscillation of the pressure gradient is predicted associated with the periodic bursts of the perturbation amplitude. Crash amplitude $\Delta A/A$ scales as $\sqrt{F_{heat}-F_{cri}}$ as is shown in Eq.(80), and the period of the oscillation becomes longer as the heating power increases.

These result are consistent with the experimental observations. In experiments of the Heliotron E device, it has been found that the oscillation of the pressure gradient occurs and that the amplitude of sawtooth-like oscillation is largest

for the first crash (Zushi, 1992). Our analysis is also consistent with the numerical simulation of the resistive interchange mode by Wakatani,et al., where sawtooth crash was recovered when the initial pressure gradient is large enough. These numerical simulation have not identified the parameter space in which the oscillatory solution exists. Our model would provide the guiding principle for the accurate numerical simulations to find out the various class of solutions.

It is noted that only the back-ground modification effect is kept in this article among various nonlinear terms. For instance, the excitation of the 2nd harmonics leads to the nonlinear term in τ such as $\tau = \tau_0 - CK$, where τ_0 is the linear growth rate and C is a constant (Sugama, et al., 1991). If this term is kept, the fixed point solution F_* becomes an increasing function of F_{heat}. However, the introduction of this term does not change the qualititive conclusion in this article. The improvement in the quantitative estimation would be expected by keeping this term.

It is also noted that the analysis in this article is highly simplified for the analytic insight. The assumption that χ and ℓ are constant in time maybe too simplified. The local pressure gradient can affect the thermal conductivity (Itoh, et al., 1992a). The current diffusivity can influence the mode growth rate for high temperature plasmas, which has a different form of $\tau[D]$ (Itoh, et al., 1992b). These problems await future study.

Acknowledgements

One of the authors acknowledge Drs. H. Zushi, K. Ichiguchi and M. Wakatani for useful discussions. This work is partly supported by the Grant-in-Aid for Scientific Research of the ministry of Education, Japan.

References

B. Carreras, L. Garcia, P. H. Diamond (1987): Phys. Fluids **30** 1388.

C. Gouldon, D. Marty, E. K. Maschke, J. P. Dumon (1968): *Plasma Physics and Controlled Nuclear Fusion Research* (IAEA, Vienna, 1968) Vol.1, p847.

J. H. Harris, O. Motojima, H. Kaneko, S. Besshou, H. Zushi, M. Wakatani, F. Sano, S. Sudo, A. Sasaki, K. Kondo, M. Sato, T. Mutoh, T. Mizuuchi, M. iima, T. Obiki, A. iiyoshi, K. Uo (1984): Phys. Rev. Lett. **53** 2242.

K. Ichiguchi, Y. Nakamura, M. Wakatani, N. Yanagi, S. Morimoto (1989): Nucl. Fusion **29** 2093.

K. Ichiguchi, Y. Nakamura, M. Wakatani (1991): Nucl. Fusion **29** 2073.

No.9 in press.

K. Itoh, S.-I. Itoh, and A. Fukuyama (1992a): Phys. Rev. Lett. **69** 1050.

K. Itoh, K. Ichiguchi, S.-I. Itoh (1992b): Phys. Fluids **B4** No.9 in press.

S. Morimoto, N. Yanagi, K. Ichiguchi, Y. Nakamura, M. Wakatani, M. Sato, T. Obiki, A. Iiyoshi (1989): Jpn. J. Appl. Phys. **28** L1470.

A. Mohri (1970): J. Phys. Soc. Jpn. **28** 1549.

A. Mohri and M. Azumi (1970): J. Phys. Soc. Jpn. **29** 1580.

M. N. Rosenbluth and C. L. Longmire (1957): Ann. Phys. **1** 120.

H. Strauss (1980): Plasma Phys. **22** 733.

H. Sugama, N. Nakajima, M. Wakatani (1991): Phys. Fluids **B3** 3290.

K. Uo (1971): Plasma Physics **13** 243.

M. Wakatani, H. Shirai, M. Yamagiwa (1984): Nucl. Fusion **24** 1407.

H. Zushi (1992): Private communications (Kyoto University).

Figure Caption

Fig. 1 Growth rate (normalized to χ/ℓ^2) as a function of the parameter D which is proportional to the pressure gradient. Parameters are chosen that $[\partial\tau/\partial D]D_c=2$ and $\ell^2 k_\theta{}^2=0.2$.

Fig. 2 Typical trajectories of three cases. (a) for the stable case, (b) for the case of asymptotic stability and (c) for the case of limit cycle. The symbol + denotes the fixed point.

Fig. 3 Regions of the saturation, damped oscillation and limit cycle solutions in the D_{heat}-z plane.

Fig. 4 Example of the temporal evolution of the pressure gradient and mode amplitude. F_{heat} is 1.05 in (a), 1.4 in (b) and 3 in (c), respectively. Temporal evolutions from the initial condition of (F, K)=(0.2, 1) (a) and (F, K)=(0.2, 0.1) (b) are shown. For (c), periodic solution is illustrated. Parameters are z=2 and $k_\theta{}^2\ell^2=0.2$.

Fig. 5 The pressure gradient as a function of the heating power, D_{heat} (a). Time average is shown by the solid line. Above the criterion for the occurence of the limit cycle solution, the time average (solid line), as well as the transient peak (dashed line) and the minimun (dotted line) are shown. Parameter is chosen as z=3.

The dependence of the mode amplitude on the heating power is shown in (b). For the limit cycle solution, the transient peak (dashed line) and the time average (solid line) are shown.

Fig.6 Period of the oscillation as a function of the heating power. Parameter is chosen as $z=5$.

Fig. 1

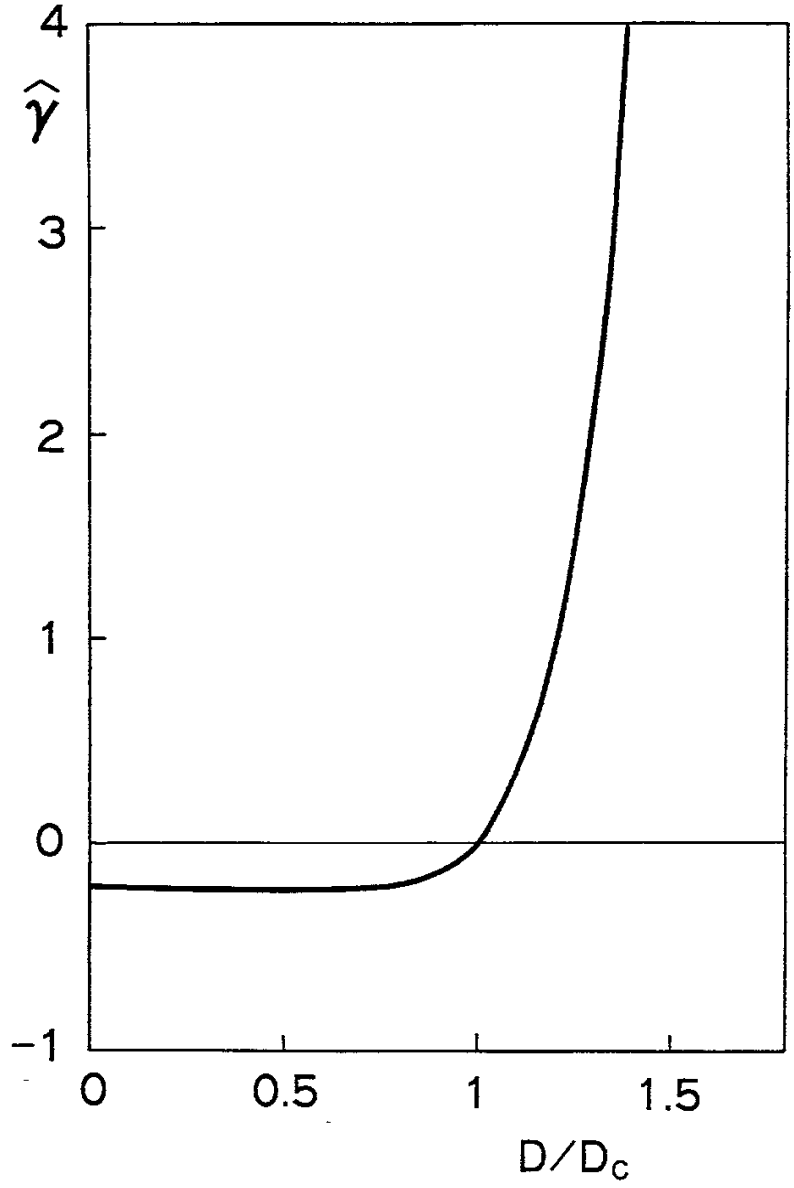

Fig. 2

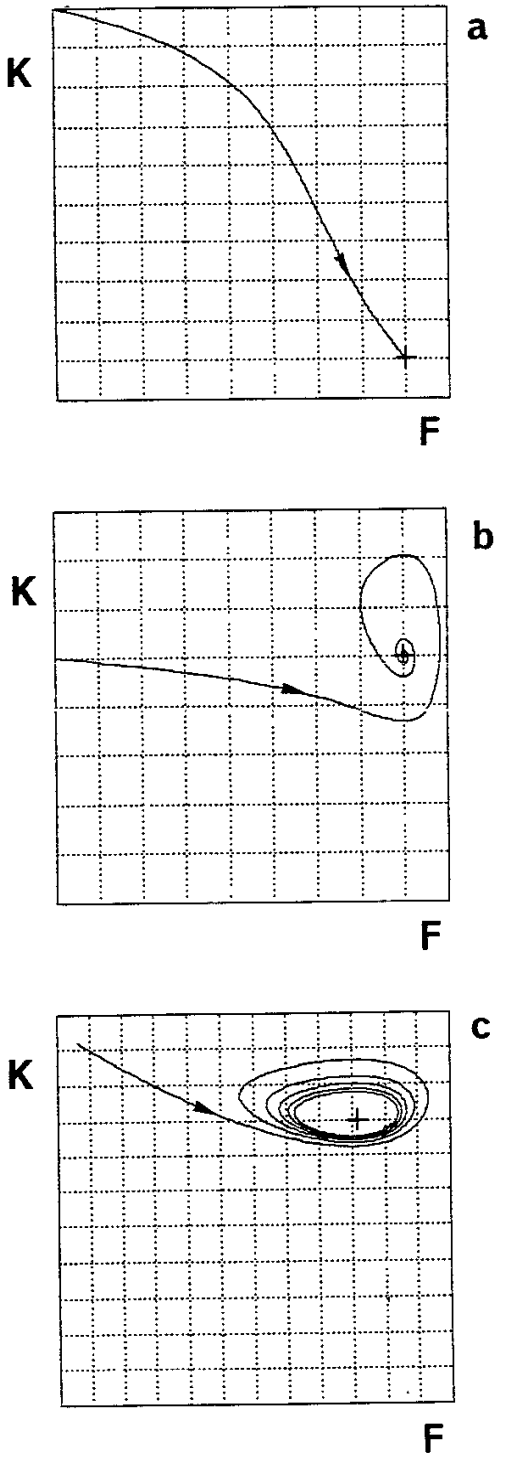

Fig. 3

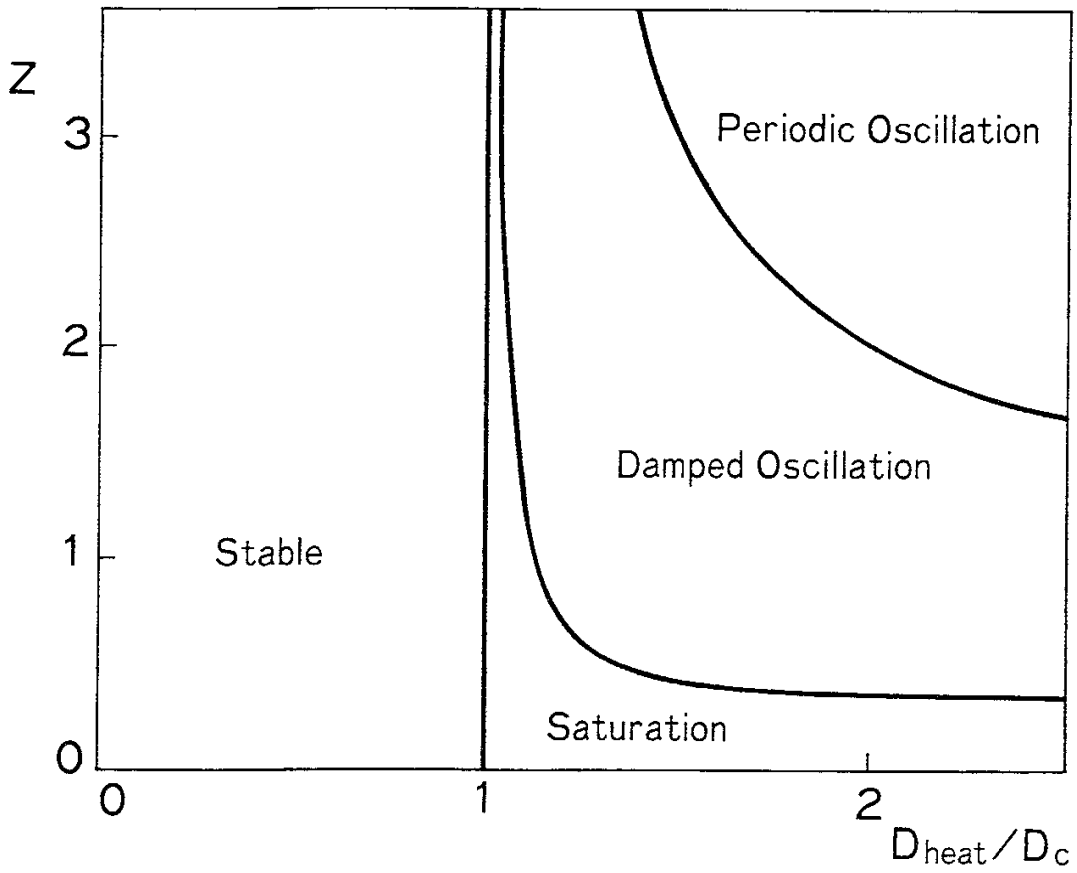
Z
3
2
1
0
Periodic Oscillation
Damped Oscillation
Stable
Saturation
0
1
2
D_{heat}/D_c

Fig. 4

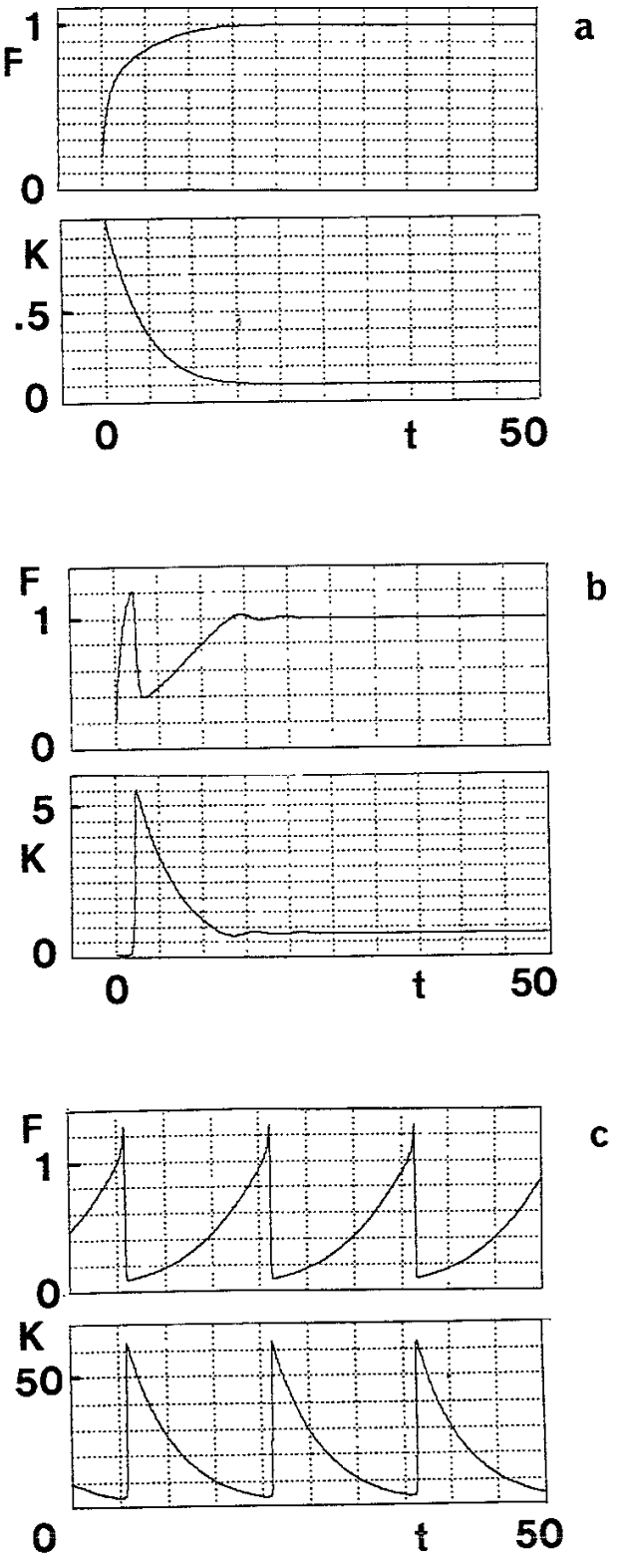

Fig.5(a)

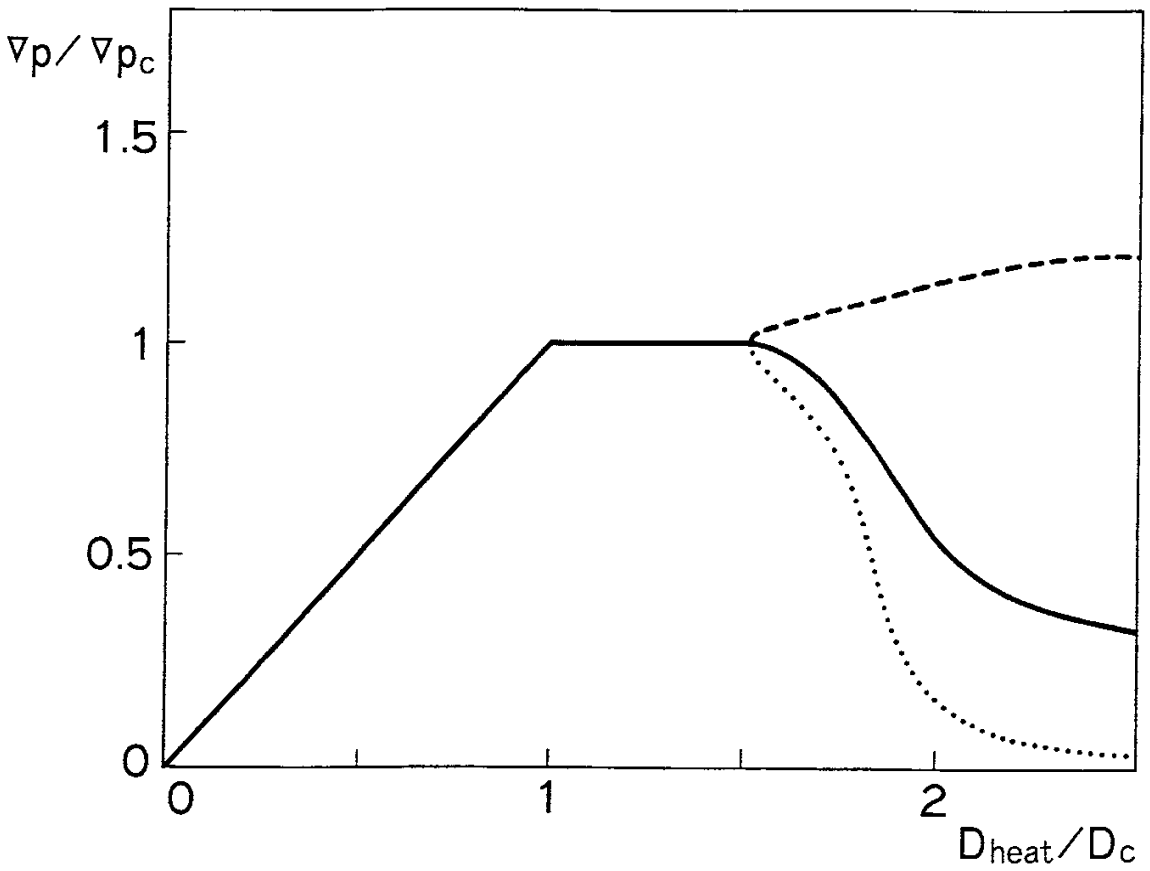

Fig.5(b)

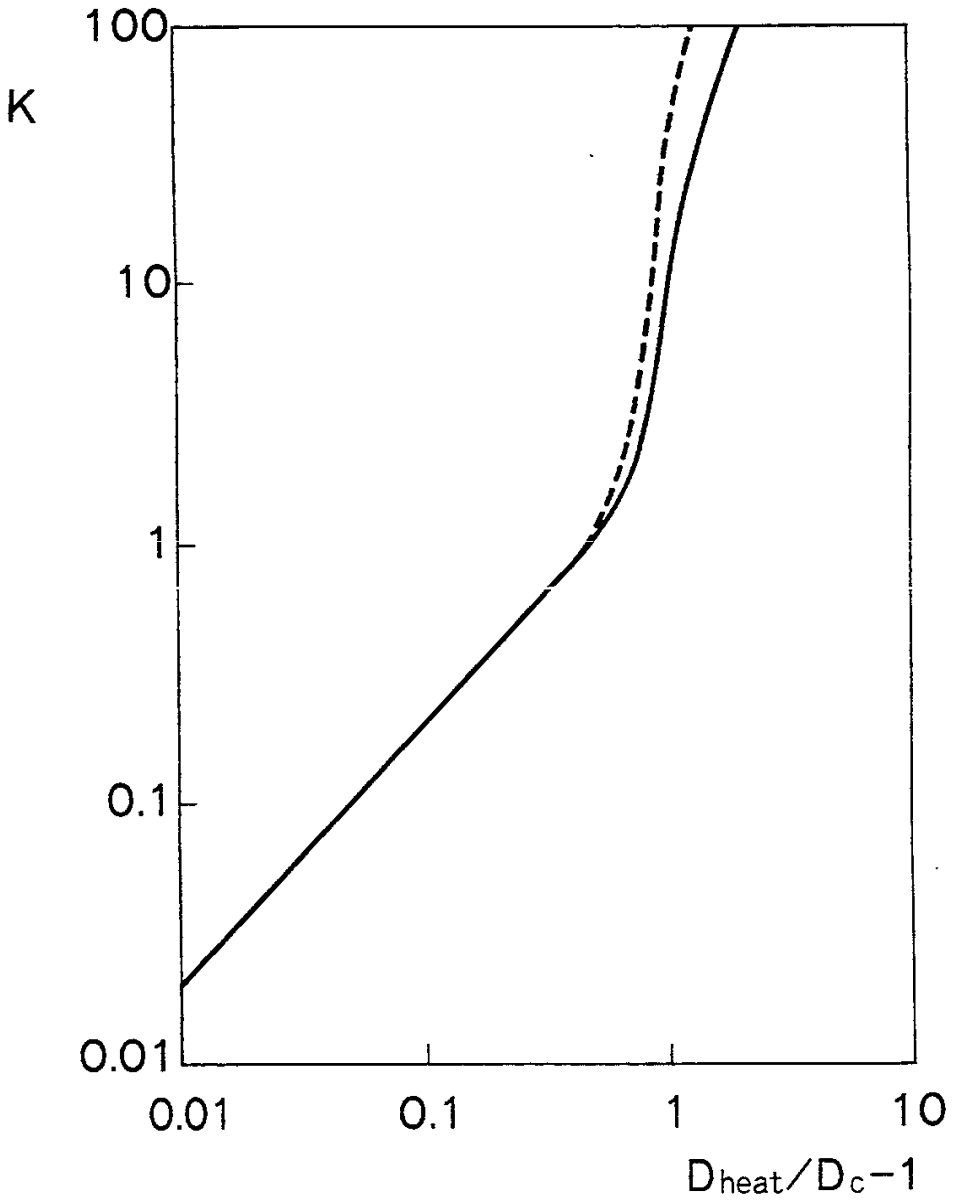

Fig. 6

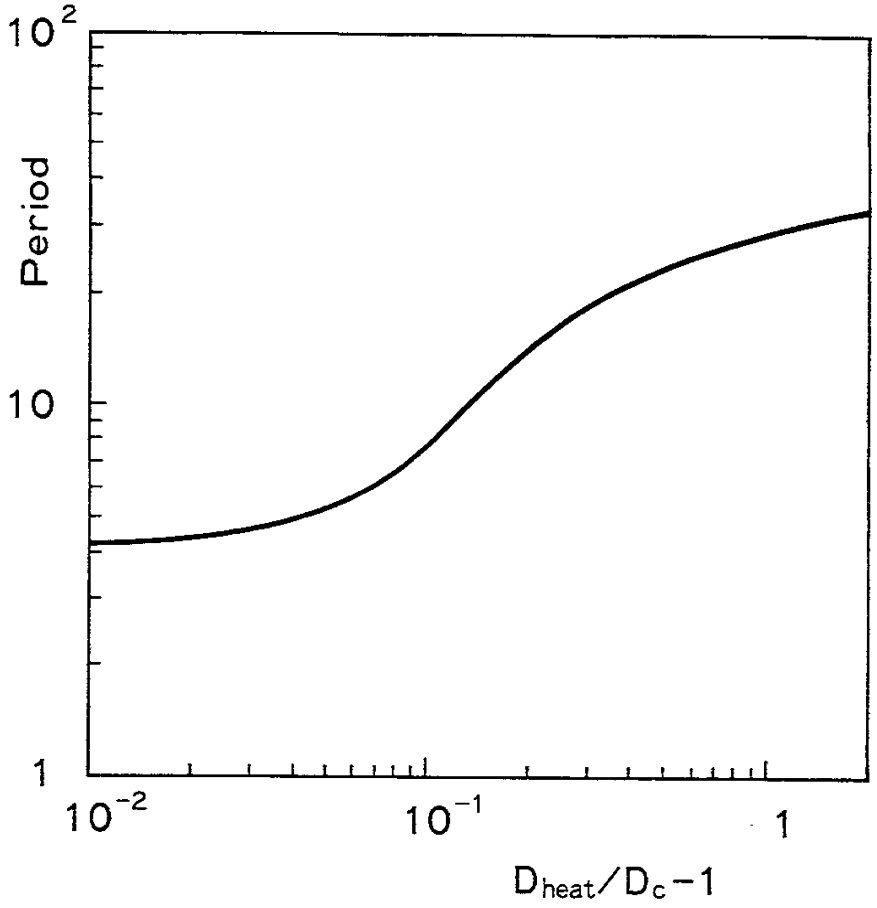

Recent Issues of NIFS Series

NIFS-146 K. Itoh, S. -I.Itoh, A. Fukuyama, S. Tsuji and Allan J. Lichtenberg, *A Model of Major Disruption in Tokamaks*; May 1992

NIFS-147 S. Sasaki, S. Takamura, M. Ueda, H. Iguchi, J. Fujita and K. Kadota, *Edge Plasma Density Reconstruction for Fast Monoenergetic Lithium Beam Probing*; May 1992

NIFS-148 N. Nakajima, C. Z. Cheng and M. Okamoto, *High-n Helicity-induced Shear Alfvén Eigenmodes*; May 1992

NIFS-149 A. Ando, Y. Takeiri, O. Kaneko, Y. Oka, M. Wada, and T. Kuroda, *Production of Negative Hydrogen Ions in a Large Multicusp Ion Source with Double-Magnetic Filter Configuration*; May 1992

NIFS-150 N. Nakajima and M. Okamoto, *Effects of Fast Ions and an External Inductive Electric Field on the Neoclassical Parallel Flow, Current, and Rotation in General Toroidal Systems*; May 1992

NIFS-151 Y. Takeiri, A. Ando, O. Kaneko, Y. Oka and T. Kuroda, *Negative Ion Extraction Characteristics of a Large Negative Ion Source with Double-Magnetic Filter Configuration*; May 1992

NIFS-152 T. Tanabe, N. Noda and H. Nakamura, *Review of High Z Materials for PSI Applications* ; Jun. 1992

NIFS-153 Sergey V. Bazdenkov and T. Sato, *On a Ballistic Method for Double Layer Regeneration in a Vlasov-Poisson Plasma*; Jun. 1992

NIFS-154 J. Todoroki, *On the Lagrangian of the Linearized MHD Equations*; Jun. 1992

NIFS-155 K. Sato, H. Katayama and F. Miyawaki, *Electrostatic Potential in a Collisionless Plasma Flow Along Open Magnetic Field Lines;* Jun. 1992

NIFS-156 O.J.W.F.Kardaun, J.W.P.F.Kardaun, S.-I. Itoh and K. Itoh, *Discriminant Analysis of Plasma Fusion Data*; Jun. 1992

NIFS-157 K. Itoh, S.-I. Itoh, A. Fukuyama and S. Tsuji, *Critical Issues and Experimental Examination on Sawtooth and Disruption Physics*; Jun. 1992

NIFS-158 K. Itoh and S.-I. Itoh, *Transition to H-Mode by Energetic Electrons*; July 1992

NIFS-159 K. Itoh, S.-I. Itoh and A. Fukuyama, *Steady State Tokamak Sustained*

by Bootstrap Current Without Seed Current; July 1992

NIFS-160 H. Sanuki, K. Itoh and S.-I. Itoh, *Effects of Nonclassical Ion Losses on Radial Electric Field in CHS Torsatron/Heliotron*; July 1992

NIFS-161 O. Motojima, K. Akaishi, K. Fujii, S. Fujiwaka, S. Imagawa, H. Ji, H. Kaneko, S. Kitagawa, Y. Kubota, K. Matsuoka, T. Mito, S. Morimoto, A. Nishimura, K. Nishimura, N. Noda, I. Ohtake, N. Ohyabu, S. Okamura, A. Sagara, M. Sakamoto, S. Satoh, T. Satow, K. Takahata, H. Tamura, S. Tanahashi, T. Tsuzuki, S. Yamada, H. Yamada, K. Yamazaki, N. Yanagi, H. Yonezu, J. Yamamoto, M. Fujiwara and A. Iiyoshi, *Physics and Engineering Design Studies on Large Helical Device*; Aug. 1992

NIFS-162 V. D. Pustovitov, *Refined Theory of Diamagnetic Effect in Stellarators;* Aug. 1992

NIFS-163 K. Itoh, *A Review on Application of MHD Theory to Plasma Boundary Problems in Tokamaks*; Aug. 1992

NIFS-164 Y.Kondoh and T.Sato, *Thought Analysis on Self-Organization Theories of MHD Plasma*; Aug. 1992

NIFS-165 T. Seki, R. Kumazawa, T. Watari, M. Ono, Y. Yasaka, F. Shimpo, A. Ando, O. Kaneko, Y. Oka, K. Adati, R. Akiyama, Y. Hamada, S. Hidekuma, S. Hirokura, K. Ida, A. Karita, K. Kawahata, Y. Kawasumi, Y. Kitoh, T. Kohmoto, M. Kojima, K. Masai, S. Morita, K. Narihara, Y. Ogawa, K. Ohkubo, S. Okajima, T. Ozaki, M. Sakamoto, M. Sasao, K. Sato, K. N. Sato, H. Takahashi, Y. Taniguchi, K. Toi and T. Tsuzuki, *High Frequency Ion Bernstein Wave Heating Experiment on JIPP T-IIU Tokamak*; Aug. 1992

NIFS-166 Vo Hong Anh and Nguyen Tien Dung, *A Synergetic Treatment of the Vortices Behaviour of a Plasma with Viscosity*; Sep. 1992

NIFS-167 K. Watanabe and T. Sato, *A Triggering Mechanism of Fast Crash in Sawtooth Oscillation*; Sep. 1992

NIFS-168 T. Hayashi, T. Sato, W. Lotz, P. Merkel, J. Nührenberg, U. Schwenn and E. Strumberger, *3D MHD Study of Helias and Heliotron;* Sep. 1992

NIFS-169 N. Nakajima, K. Ichiguchi, K. Watanabe, H. Sugama, M. Okamoto, M. Wakatani, Y. Nakamura and C. Z. Cheng, *Neoclassical Current and Related MHD Stability, Gap Modes, and Radial Electric Field Effects in Heliotron and Torsatron Plasmas;* Sep. 1992

NIFS-170 H. Sugama, M. Okamoto and M. Wakatani, *K- ε Model of Anomalous Transport in Resistive Interchange Turbulence* ; Sep, 1992

NIFS-171 H. Sugama, M. Okamoto and M. Wakatani, *Vlasov Equation in the Stochastic Magnetic Field* ; Sep. 1992

NIFS-172 N. Nakajima, M. Okamoto and M. Fujiwara, *Physical Mechanism of E_ϕ-Driven Current in Asymmetric Toroidal Systems* ; Sep.1992

NIFS-173 N. Nakajima, J. Todoroki and M. Okamoto, *On Relation between Hamada and Boozer Magnetic Coordinate System* ; Sep. 1992

NIFS-174 K. Ichiguchi, N. Nakajima, M. Okamoto, Y. Nakamura and M. Wakatani, *Effects of Net Toroidal Current on Mercier Criterion in the Large Helical Device* ; Sep. 1992

NIFS-175 S. -I. Itoh, K. Itoh and A. Fukuyama, *Modelling of ELMs and Dynamic Responses of the H-Mode* ; Sep. 1992

NIFS-176 K. Itoh, S.-I. Itoh, A. Fukuyama, H. Sanuki, K. Ichiguchi and J. Todoroki, *Improved Models of β-Limit, Anomalous Transport and Radial Electric Field with Loss Cone Loss in Heliotron / Torsatron* ; Sep. 1992

NIFS-177 N. Ohyabu, K. Yamazaki, I. Katanuma, H. Ji, T. Watanabe, K. Watanabe, H. Akao, K. Akaishi, T. Ono, H. Kaneko, T. Kawamura, Y. Kubota, N. Noda, A. Sagara, O. Motojima, M. Fujiwara and A. Iiyoshi, *Design Study of LHD Helical Divertor and High Temperature Divertor Plasma Operation* ; Sep. 1992

NIFS-178 H. Sanuki, K. Itoh and S.-I. Itoh, *Selfconsistent Analysis of Radial Electric Field and Fast Ion Losses in CHS Torsatron / Heliotron* ; Sep. 1992

NIFS-179 K. Toi, S. Morita, K. Kawahata, K. Ida, T. Watari, R. Kumazawa, A. Ando, Y. Oka, K. Ohkubo, Y. Hamada, K. Adati, R. Akiyama, S. Hidekuma, S. Hirokura, O. Kaneko, T. Kawamoto, Y. Kawasumi, M. Kojima, T. Kuroda, K. Masai, K. Narihara, Y. Ogawa, S. Okajima, M. Sakamoto, M. Sasao, K. Sato, K. N. Sato, T. Seki, F. Shimpo, S. Tanahashi, Y. Taniguchi, T. Tsuzuki, *New Features of L-H Transition in Limiter H-Modes of JIPP T-IIU* ; Sep. 1992

NIFS-180 H. Momota, Y. Tomita, A. Ishida, Y. Kohzaki, M. Ohnishi, S. Ohi, Y. Nakao and M. Nishikawa, *D-^{3}He Fueled FRC Reactor "Artemis-L"* ; Sep. 1992

NIFS-181 T. Watari, R. Kumazawa, T. Seki, Y. Yasaka, A. Ando, Y. Oka, O. Kaneko, K. Adati, R. Akiyama, Y. Hamada, S. Hidekuma, S. Hirokura, K. Ida, K. Kawahata, T. Kawamoto, Y. Kawasumi, S. Kitagawa, M. Kojima, T. Kuroda, K. Masai, S. Morita, K. Narihara,

Y. Ogawa, K. Ohkubo, S. Okajima, T. Ozaki, M. Sakamoto, M. Sasao, K. Sato, K. N. Sato, F. Shimpo, H. Takahashi, S. Tanahasi, Y. Taniguchi, K. Toi, T. Tsuzuki and M. Ono, *The New Features of Ion Bernstein Wave Heating in JIPP T-IIU Tokamak*; Sep, 1992

NIFS-182 K. Itoh, H. Sanuki and S.-I. Itoh, *Effect of Alpha Particles on Radial Electric Field Structure in Torsatron / Heliotron Reactor*; Sep. 1992

NIFS-183 S. Morimoto, M. Sato, H. Yamada, H. Ji, S. Okamura, S. Kubo, O. Motojima, M. Murakami, T. C. Jernigan, T. S. Bigelow, A. C. England, R. S. Isler, J. F. Lyon, C. H. Ma, D. A. Rasmussen, C. R. Schaich, J. B. Wilgen and J. L. Yarber, *Long Pulse Discharges Sustained by Second Harmonic Electron Cyclotron Heating Using a $35GH_Z$ Gyrotron in the Advanced Toroidal Facility*; Sep. 1992

NIFS-184 S. Okamura, K. Hanatani, K. Nishimura, R. Akiyama, T. Amano, H. Arimoto, M. Fujiwara, M. Hosokawa, K. Ida, H. Idei, H. Iguchi, O. Kaneko, T. Kawamoto, S. Kubo, R. Kumazawa, K. Matsuoka, S. Morita, O. Motojima, T. Mutoh, N. Nakajima, N. Noda, M. Okamoto, T. Ozaki, A. Sagara, S. Sakakibara, H. Sanuki, T. Saki, T. Shoji, F. Shimbo, C. Takahashi, Y. Takeiri, Y. Takita, K. Toi, K. Tsumori, M. Ueda, T. Watari, H. Yamada and I. Yamada, *Heating Experiments Using Neutral Beams with Variable Injection Angle and ICRF Waves in CHS* ; Sep. 1992

NIFS-185 H. Yamada, S. Morita, K. Ida, S. Okamura, H. Iguchi, S. Sakakibara, K. Nishimura, R. Akiyama, H. Arimoto, M. Fujiwara, K. Hanatani, S. P. Hirshman, K. Ichiguchi, H. Idei, O. Kaneko, T. Kawamoto, S. Kubo, D. K. Lee, K. Matsuoka, O, Motojima, T. Ozaki, V. D. Pustovitov, A. Sagara, H. Sanuki, T. Shoji, C. Takahashi, Y. Takeiri, Y. Takita, S. Tanahashi, J. Todoroki, K. Toi, K. Tsumori, M. Ueda and I. Yamada, *MHD and Confinement Characteristics in the High-β Regime on the CHS Low-Aspect-Ratio Heliotron / Torsatron* ; Sep. 1992

NIFS-186 S. Morita, H. Yamada, H. Iguchi, K. Adati, R. Akiyama, H. Arimoto, M. Fujiwara, Y. Hamada, K. Ida, H. Idei, O. Kaneko, K. Kawahata, T. Kawamoto, S. Kubo, R. Kumazawa, K. Matsuoka, T. Morisaki, K. Nishimura, S. Okamura, T. Ozaki, T. Seki, M. Sakurai, S, Sakakibara, A. Sagara, C. Takahashi, Y. Takeiri, H. Takenaga, Y. Takita, K. Toi, K. Tsumori, K. Uchino, M. Ueda, T. Watari, I. Yamada, *A Role of Neutral Hydrogen in CHS Plasmas with Reheat and Collapse and Comparison with JIPP T-IIU Tokamak Plasmas* ; Sep. 1992

NIFS-187 K. Ioth, S.-I. Itoh, A. Fukuyama, M. Yagi and M. Azumi, *Model of the L-Mode Confinement in Tokamaks* ; Sep. 1992